Solving the bound-state Schrödinger equation by reproducing kernel interpolation

Xu-Guang Hu, Tak-San Ho, and Herschel Rabitz
Department of Chemistry, Princeton University, Princeton, New Jersey 08544-1009
(Received 16 November 1998)

Based on reproducing kernel Hilbert space theory and radial basis approximation theory, a grid method is developed for numerically solving the *N*-dimensional bound-state Schrödinger equation. Central to the method is the construction of an appropriate bounded reproducing kernel (RK) $\Lambda_\alpha(\|\mathbf{r}\|)$ from the linear operator $-\nabla_{\mathbf{r}}^2+\lambda^2$ where $\nabla_{\mathbf{r}}^2$ is the *N*-dimensional Laplacian, $\lambda>0$ is a parameter related to the binding energy of the system under study, and the real number $\alpha>N$. The proposed (Sobolev) RK $\Lambda_\alpha(\mathbf{r},\mathbf{r}')$ is shown to be a positive-definite radial basis function, and it matches the asymptotic solutions of the bound-state Schrödinger equation. Numerical tests for the one-dimensional (1D) Morse potential and 2D Henon-Heiles potential reveal that the method can accurately and efficiently yield all the energy levels up to the dissociation limit. Comparisons are also made with the results based on the distributed Gaussian basis method in the 1D case as well as the distributed approximating functional method in both 1D and 2D cases.

PACS number(s): 02.70.−c, 02.60.Lj, 02.60.Ed, 03.65.Ge

I. INTRODUCTION

The function approximation scheme from which different methods can be characterized is of fundamental importance in numerically solving ordinary or partial differential equations. Two commonly used function approximation schemes are interpolation (e.g., polynomial interpolation and spline interpolation, etc.) and basis function expansion (e.g., Fourier series and generalized Fourier series, etc.). The former are identified as grid methods which are either global or local, whereas the latter are referred to as spectral methods which are global. Both global and local approaches have their own strong and weak points depending on the practical application. Generally speaking, global approaches such as Fourier series, orthogonal polynomial expansions and polynomial interpolation produce more accurate results than local ones in comparable settings. However, local approaches such as finite element and finite difference are more flexible and are easier to implement than global ones for systems with complex boundary conditions. In this paper we will focus on the interpolation scheme for function approximations in solving the bound-state Schrödinger equation.

The quality of an interpolation scheme is closely related to not only the nature of interpolator but also the total number of interpolating points (i.e., grid points) and their distribution. For polynomial interpolators, grid point distribution can in principle be quite arbitrary as long as they are distinct. Nevertheless, Shannon's sampling theorem based on a special interpolation function $\sin(x)/x$ can only accept evenly spaced grid points using the zeros of $\sin(x)$ on the real axis. In recent years, there has been considerable interest in grid methods for solving the time-dependent or time-independent Schrödinger equations [1], among which are the discrete variable representation (DVR) [2–8], the Fourier pseudospectral method [9,10], the distributed Gaussian (DGB) basis method [11–15], and the distributed approximating functionals (DAF) [16,17,19].

DVR and Fourier pseudospectral methods using orthogonal basis sets are well defined in one-dimensional cases. Both methods necessitate quadrature points, i.e., zeros of orthogonal basis functions (e.g., orthogonal polynomials and trigonometric functions, etc.), as their interpolating nodal points. For more than one-dimensional cases, however, the tensor product form of one-dimensional basis sets are usually adopted. Although the tensor product form is a conceptually simple way to construct multidimensional orthogonal basis sets, it is neither efficient nor accurate as a numerical scheme because the total number of quadrature points will drastically increase with dimension, thus causing computer storage, code execution time, and numerical instability problems.

Shizgal [6] and Schneider [7] have modified the DVR methods by using one-dimensional nonclassical polynomials. Both methods have a notable feature that builds the correct boundary conditions and asymptotic behavior of the system under study into their polynomial constructions and, thus not only reduces the number of quadrature points employed but also raises the accuracy in numerical calculations. Notwithstanding these attractive features, for more than one-dimensional problems, both methods need to employ the tensor product ansatz.

The DAF method developed by Kouri and co-workers [16,17,19], is another systematic way to incorporate a (quadrature) weight function corresponding to a classical polynomial into function approximations over the distributed grids. The typical interpolating and noninterpolating DAF procedures employ Hermite polynomials and their Gaussian weight and have been successfully applied to solve one- and two-dimensional bound-state Schrödinger equations and, one-dimensional Fokker-Planck equations [16–18]. In principle, the DAF method as an off-spring of the moving least square treatment, can use any kind of grid point distributions, but in practice, only uniformly distributed ones along each dimension have been well explored to avoid the need to invert a matrix formed on the grids [19]. Otherwise, the DAF method would become computationally costly for more than one-dimensional problems because of the matrix inversion. As a result, the tensor product form is the only viable choice for the DAF method to be extended to multidimensional applications.

The DGB method has been widely used in molecular vibration-rotational calculations [11–15]. One advantage of using the Gaussian function $\exp(-\lambda\|\mathbf{r}\|^2)(\lambda>0)$ as an inter-

polation basis function on grids is that the relevant potential matrix elements can be accurately evaluated using low order Gauss-Hermite quadratures. Furthermore, the grid points can be flexibly distributed over configuration regions where the amplitude of the wave function is significant. This latter feature allows for the symmetry of the system under study to be built into the grid point distribution. Finally, the Gaussian function, similar to the Sobolev reproducing kernel (RK) function $\Lambda_\alpha(\|\mathbf{r}\|)$ introduced in the paper, is a radial basis function with respect to its argument. All radial basis functions can be arbitrarily distributed, thus, allowing for a great reduction of the total number of grid points to be employed in the calculations.

The reproducing kernel Hilbert space (RKHS) method has been shown to be a powerful tool for constructing accurate analytical potential energy hypersurfaces [20–22] and for solving the bound-state Schrödinger equation [23]. In the former case the RKHS and its associated RK were constructed from Taylor's formula with exact remainder, whereas in the latter case they were constructed from the Green's function corresponding to the bound-state Schrödinger equation. These two RK's belong to a class of generalized spline functions associated with ordinary linear differential operators, but subject to different boundary conditions [24–26]. In this paper we pursue the use of the RKHS method for solving the bound-state Schrödinger equation by generalizing the previous definition of the RK [23]. The RKHS method along with the interpolation properties of radial basis functions [25,27,28] underlies this development. The central idea of the method is to define a Hilbert space with a suitable inner product from which an appropriate positive-definite RK can be constructed uniquely [26]. In this paper, an N-dimensional RK $\Lambda_\alpha(\|\mathbf{r}\|)$ is constructed from the linear operator $-\nabla_{\mathbf{r}}^2+\lambda^2$ where $\nabla_{\mathbf{r}}^2$ is the N-dimensional Laplacian, $\lambda>0$ is a parameter related to the binding energy of the system under study, and the real number $\alpha>N$. The proposed (Sobolev) $\Lambda_\alpha(\|\mathbf{r}\|)$ RK is shown to be a positive-definite radial basis function (RBF), and it matches the asymptotic solutions of the bound-state Schrödinger equation.

The specific radial property of the Sobolev RK $\Lambda_\alpha(\|\mathbf{r}\|)$ can be incorporated into an efficient and accurate interpolation scheme for approximating the bound-state wave function $\psi(\mathbf{r})$. Recently, RBF interpolation has attracted a great deal of interest in approximation theory for multivariate scattered data interpolation [27,28]. There are three salient features in using this theory for the grid method: (1) the only restriction required for the distribution of grid points is that every point must be distinct from one another. (2) The RBF's need to be symmetric and strictly or conditionally positive-definite. Each RBF always generates an RKHS with a proper inner product such that the reproducing property holds [33]. (3) A function can be optimally recovered from scattered data by the RBF interpolation [27,28,33,34].

The paper is organized as follows. In Sec. II the underlying principle of the RKHS method and its applications to scattered data interpolation and function approximation are presented for general multidimensional cases. In Sec. III the numerical implementation is illustrated by solving the Schrödinger equation for a one-dimensional (1D) Morse potential as well as a two-dimensional Henon-Heiles potential. Comparisons are also made with the results based on the distributed Gaussian basis method in the 1D case as well as the distributed approximating functional method in both 1D and 2D cases. Concluding remarks are given in Sec. IV.

II. THEORY

A. RKHS and RK

Without loss of generality we start with the N-dimensional Schrödinger equation in atomic units:

$$\left\{-\sum_{i=1}^{N}\frac{1}{2\mu_i}\frac{\partial^2}{\partial x_i^2}+V(x_1,x_2,\ldots,x_N)\right\}\psi(x_1,x_2,\ldots,x_N)=E\psi(x_1,x_2,\ldots,x_N). \tag{1}$$

The total energy of the system E is assumed to be negative for the bound-state problems considered in this paper. By adopting the coordinates $z_i=\sqrt{\mu_i}x_i(i=1,2,\ldots N)$, Eq. (1) reduces to

$$(-\nabla_{\mathbf{r}}^2+\lambda^2)\psi(\mathbf{r})=-2V(\mathbf{r})\psi(\mathbf{r}), \tag{2}$$

where $\lambda^2=-2E>0$ and $\nabla_{\mathbf{r}}^2=\Sigma_{i=1}^{N}(d^2/dz_i^2)$ with $\mathbf{r}$ being understood to designate a N-dimensional (ND) vector for $(z_1,z_2,\ldots,z_N)$ collectively. Based on the Green's function $G(\mathbf{r},\mathbf{r}')$ for the linear operator $\hat{M}(\mathbf{r})=-\nabla_{\mathbf{r}}^2+\lambda^2$, Eq. (2) can be readily transformed into an integral equation

$$\psi(\mathbf{r})=\int_{\mathbb{R}^N}d\mathbf{r}'\,G(\mathbf{r},\mathbf{r}')[-2V(\mathbf{r}')]\psi(\mathbf{r}'), \tag{3}$$

where $\mathbb{R}^N$ denotes the entire ND Euclidean space. The positive-definite Green's function $G(\mathbf{r},\mathbf{r}')$ satisfies the correct bound-state boundary conditions and it has an explicit form expressed in terms of the modified Bessel function of the third kind $K_\nu(z)$

$$G(\mathbf{r},\mathbf{r}')=\frac{1}{\lambda}\left(\frac{\lambda}{2\pi}\right)^{N/2}\frac{K_{N/2-1}(\lambda\|\mathbf{r}-\mathbf{r}'\|)}{\|\mathbf{r}-\mathbf{r}'\|^{N/2-1}}, \tag{4}$$

where $\|\cdots\|$ represents the Euclidean norm, i.e., the Euclidean distance. Within the framework of Eqs. (3) and (4) Kalos has carried out Monte Carlo calculations for the ground state of some few-body systems [29]. The linear operator $\hat{M}(\mathbf{r})=-\nabla_{\mathbf{r}}^2+\lambda^2$ with $\lambda^2>0$ and its Green's function $G(\mathbf{r},\mathbf{r}')$ also underlie the RKHS method presented below for general multidimensional bound-state problems. We first present some basic concepts involved in the RKHS and RK [25,26].

Let $\mathbf{H}$ be a Hilbert space formed by a class of real continuous bounded functions. The Hilbert space $\mathbf{H}$ is said to be a reproducing kernel Hilbert space (RKHS) if there exists a real symmetric and positive-definite function $K(t,t')$ which, for every t', $K(t,t')$ as a function of t, belongs to $\mathbf{H}$, and possesses the following reproducing property

$$f(t)=\langle f(t'),K(t,t')\rangle_{t'},\qquad K(t,s)=\langle K(t,t'),K(s,t')\rangle_{t'}, \tag{5}$$

where $f(t)$ is a function in $\mathbf{H}$ and $K(t,t')$ is called the reproducing kernel (RK) of $\mathbf{H}$. The explicit definition of the nature of the inner product $\langle \cdots, \cdots \rangle_{t'}$ will depend on the particular linear space involved, and the subscript t' indicates that the inner product is performed over functions of t'. Intuitively, a reproducing kernel Hilbert space is one which contains a kernel function $K(t,t')$ playing a role similar to the Dirac delta function $\delta(t-t')$. However, the Dirac delta function is not truly a reproducing kernel. For example, for an L^2 Hilbert space formed by a class of square integrable functions, although the Dirac delta function $\delta(t-t')$ possesses the reproducing property $\int dt' \delta(t-t')f(t')=f(t)$, it does not satisfy the criterion that, for every t', $\delta(t-t')$ as a function of t belongs to the same Hilbert space. It can be shown [26] that, to every RKHS there corresponds a unique RK and, conversely, given a real symmetric and positive-definite function $K(t,t')$ one can construct a unique RKHS with $K(t,t')$ as its RK. In general, the construction of a RKHS is dependent on both the class of functions forming a linear space and the definition of the associated inner product. To establish a RKHS for solving the bound-state Schrödinger equation, the associated RK must be at least twice continuously differentiable and square integrable (in accordance with the bounded nature of bound-state wave functions).

For an illustration, we first consider the construction of suitable RK's for the 1D bound-state case. It is easy to show that by the use of the 1D Green's function $G(z,z')$ of the linear operator $\hat{M}(z')=-d^2/dz^2+\lambda^2$, the kernel function

$$\Lambda(z,z') = \int_{-\infty}^{+\infty} dz'' G(z,z'')G(z'',z')$$

$$= \frac{1}{4\lambda^3}(1+\lambda|z-z'|)e^{-\lambda|z-z'|}, \tag{6}$$

is square integrable for any given z (or z') as well as real symmetric positive definite. Furthermore, the action of the operator $\hat{M}(z')$ on the $\Lambda(z,z')$ yields

$$\hat{M}(z')\Lambda(z,z') = \int_{-\infty}^{+\infty} dz'' G(z,z'')\{\hat{M}(z')G(z'',z')\}$$

$$= \int_{-\infty}^{+\infty} dz'' G(z,z'')\delta(z''-z') = G(z,z'). \tag{7}$$

Here, we have used the property $\hat{M}(z')G(z'',z')=\delta(z''-z')$. If the parameter λ in Eq. (6) is determined by the Schrödinger Eq. (2), then, the integral Eq. (3), can be converted, in terms of Eqs. (2) and (7), to another important form

$$\psi(z) = \int_{-\infty}^{+\infty} dz' \{\hat{M}(z')\Lambda(z,z')\}\{\hat{M}(z')\psi(z')\}. \tag{8}$$

We remark that this relation should not be taken as an integral equation for determining the wave function $\psi(z)$ as it does not involve the potential of the system. It is merely an identity satisfied by any $\psi(z)$ that solves the Schrödinger Eq. (2) with any acceptable potential $V(z)$. Of paramount importance is that Eq. (8) enables one to define an appropriate RKHS for the 1D bound-state problem, as seen below.

Suppose that a class of square-integrable continuous functions $\{\psi, \phi, \ldots\}$, forms a linear Hilbert space which endows an inner product and norm defined as

$$\langle \phi, \psi \rangle = \int_{-\infty}^{+\infty} dz \{\hat{M}(z)\phi(z)\}^*\{\hat{M}(z)\psi(z)\},$$

$$\langle \psi, \psi \rangle = \|\psi\|^2 < \infty. \tag{9}$$

where the * means the Hermitian conjugate. The RK corresponding to this Hilbert space is uniquely given by $\Lambda(z,z')$ defined in Eq. (6). The reproducing property can be easily seen from the following manipulations:

$$\psi(z) = \langle \Lambda(z,z'), \psi(z') \rangle_{z'}$$

$$= \int_{-\infty}^{+\infty} dz' \{\hat{M}(z')\Lambda(z,z')\}^*\{\hat{M}(z')\psi(z')\}$$

$$= \int_{-\infty}^{+\infty} dz' G(z,z')^*\{\hat{M}(z')\psi(z')\}$$

$$= \int_{-\infty}^{+\infty} dz' \{\hat{M}(z')G(z,z')\}^*\psi(z')$$

$$= \int_{-\infty}^{+\infty} dz' \delta(z-z')\psi(z'), \tag{10}$$

where the Hermiticity of the operator $\hat{M}(z)$ has been used. Note that the last equality does not imply that the δ function is a RK because the definition of the inner product is different from Eq. (9) and the usual L^2 Hilbert space with $\hat{M}(z)=1$ is not a RKHS. In general, a null linear subspace spanned by the set of functions fulfilling the equation $\hat{M}(z)f(z)=0$ needs to be added to the RKHS for completion. However, here this null space only has the trivial solution $f(z)=0$ satisfying square integrability.

It is easy to see that the Hilbert space endowed with the inner product (9) will reduce to the usual L^2 Hilbert space endowed with the inner product $\int_{-\infty}^{+\infty} dz \phi^*(z)\psi(z)$ by taking $\hat{M}(z)=1$. Although both Hilbert spaces are all composed of square-integrable functions, the present (Sobolev) Hilbert space excludes functions with differentiability of less than second order, such as the Heaviside step function, thus imposing more stringent smoothness conditions on its members than its L^2 counterpart. The solutions of the bound-state Schrödinger equation are required to be at least twice continuously differentiable and will definitely fall into the present Hilbert space which is a subspace of the usual L^2 Hilbert space.

In a previous paper [23] the above 1D RK has been adopted for variationally solving the 1D bound-state Schrödinger equation in conjunction with a grid method. The numerical results showed that the RK $\Lambda(z,z')$ defined in Eq. (6) as an interpolation basis can yield accurate energy levels up to the dissociation limit for the Morse and Pöschl-Teller potentials. A major drawback with the above RK is its lack

of differentiability to high orders, as a result, more grid points are needed in the corresponding calculations. Nevertheless, the above formulation is closely related to the asymptotic form $\hat{M}(z)$ of the bound-state Schrödinger operator and the associated Green's function $G(z,z')$. This property renders the RKHS method accurate even up to the dissociation limit. Unfortunately, the above procedure for constructing the 1D RKHS and its associated RK cannot be directly extended beyond the 1D case because the resultant RK's are not necessarily square integrable (as can be seen from the following development and the Appendix).

In the following we describe a different procedure based on Fourier analysis that enables the construction of suitable RK's for general multidimensional bound-state problems. We first define a positive-definite operator $\hat{Q}(\mathbf{r})=\hat{M}(\mathbf{r})^{\alpha/4}=(-\nabla^2+\lambda^2)^{\alpha/4}$ with $\lambda^2>0$, $\alpha>0$ and assume the existence of its Fourier transform [30] through the relation

$$\hat{Q}(\mathbf{r})\psi(\mathbf{r})=\hat{M}(\mathbf{r})^{\alpha/4}\psi(\mathbf{r})=\frac{1}{(2\pi)^N}\int_{\mathbb{R}^N}d\mathbf{k}(\lambda^2+\mathbf{k}^2)^{\alpha/4}\times\tilde{\psi}(\mathbf{k})e^{i\mathbf{k}\cdot\mathbf{r}}, \tag{11}$$

where $\tilde{\psi}$ is the Fourier transform of ψ. The operator $\hat{Q}(\mathbf{r})$ thus defined is Hermitian provided that $\hat{Q}(\mathbf{r})\psi(\mathbf{r})$ is square integrable, leading to a real Hilbert (Sobolev) space $\mathbf{H}_\alpha$ which is endowed with the inner product and norm

$$\begin{aligned}\langle\phi,\psi\rangle&=\int_{\mathbb{R}^N}d\mathbf{r}\{\hat{Q}(\mathbf{r})\phi(\mathbf{r})\}^*\{\hat{Q}(\mathbf{r})\psi(\mathbf{r})\}\\&=\int_{\mathbb{R}^N}d\mathbf{r}\{\hat{M}(\mathbf{r})^{\alpha/4}\phi(\mathbf{r})\}^*\{\hat{M}(\mathbf{r})^{\alpha/4}\psi(\mathbf{r})\}\\&=\frac{1}{(2\pi)^N}\int_{\mathbb{R}^N}d\mathbf{k}\tilde{\phi}(\mathbf{k})^*\tilde{\psi}(\mathbf{k})(\lambda^2+\mathbf{k}^2)^{\alpha/2}\end{aligned}$$

$$\langle\psi,\psi\rangle=\|\psi\|^2<\infty, \tag{12}$$

for any functions ψ and ϕ belonging to $\mathbf{H}_\alpha$. The L^2 square-integrability of $\hat{Q}(\mathbf{r})\psi(\mathbf{r})$, while ensuring that of ψ in the present Hilbert space $\mathbf{H}_\alpha$, removes those functions for which $\hat{Q}(\mathbf{r})\psi(\mathbf{r})$'s are not L^2 square integrable from the usual L^2 Hilbert space. Once the inner product is given, we can proceed to construct the unique RK associated with Hilbert space $\mathbf{H}_\alpha$.

There are two ways to construct bounded RK's with the restriction of $\alpha>N$ (to be addressed below). One approach is to follow the same procedure as the above 1D example by first finding the Green's function of the operator $\hat{Q}(\mathbf{r})=(-\nabla_{\mathbf{r}}^2+\lambda^2)^{\alpha/4}$ with proper bound-state boundary conditions and then convolving the Green's function, as in Eq. (6), to achieve the desired RK. This way is conventional, but not straightforward as mentioned previously. Another approach presented below is much easier and conceptually more appealing.

Let $\Lambda_\alpha(\mathbf{r},\mathbf{r}')$ be the required RK associated with the above Hilbert space $\mathbf{H}_\alpha$ and $\tilde{\Lambda}_\alpha(\mathbf{r},\mathbf{k})$ be its Fourier transform related by

$$\tilde{\Lambda}_\alpha(\mathbf{r},\mathbf{k})=\int_{\mathbb{R}^N}d\mathbf{r}'\Lambda_\alpha(\mathbf{r},\mathbf{r}')e^{-i\mathbf{k}\cdot\mathbf{r}'}. \tag{13}$$

The reproducing property of $\Lambda_\alpha(\mathbf{r},\mathbf{r}')$ under the inner product (12) will manifest itself, if and only if

$$\tilde{\Lambda}_\alpha(\mathbf{r},\mathbf{k})=(\lambda^2+\mathbf{k}^2)^{-\alpha/2}e^{-i\mathbf{k}\cdot\mathbf{r}}. \tag{14}$$

Thus, any function $\psi(\mathbf{r})$ belonging to $\mathbf{H}_\alpha$ can be written as

$$\begin{aligned}\psi(\mathbf{r})&=\langle\Lambda_\alpha(\mathbf{r},\mathbf{r}'),\psi(\mathbf{r}')\rangle_{\mathbf{r}'}\\&=\frac{1}{(2\pi)^N}\int_{\mathbb{R}^N}d\mathbf{k}\tilde{\Lambda}_\alpha(\mathbf{r},\mathbf{k})^*\tilde{\psi}(\mathbf{k})(\lambda^2+\mathbf{k}^2)^{\alpha/2}\\&=\frac{1}{(2\pi)^N}\int_{\mathbb{R}^N}d\mathbf{k}\tilde{\psi}(\mathbf{k})e^{i\mathbf{k}\cdot\mathbf{r}}.\end{aligned} \tag{15}$$

The last equality in Eq. (15) is just the inverse Fourier transform of the function $\tilde{\psi}(\mathbf{k})$. As a result, the required RK can be directly constructed by the inverse Fourier transform of $\tilde{\Lambda}_\alpha(\mathbf{r},\mathbf{k})$ as

$$\begin{aligned}\Lambda_\alpha(\mathbf{r},\mathbf{r}')&=\frac{1}{(2\pi)^N}\int_{\mathbb{R}^N}d\mathbf{k}\tilde{\Lambda}_\alpha(\mathbf{r}',\mathbf{k})e^{i\mathbf{k}\cdot\mathbf{r}}\\&=\frac{1}{(2\pi)^N}\int_{\mathbb{R}^N}d\mathbf{k}\frac{e^{i\mathbf{k}\cdot(\mathbf{r}-\mathbf{r}')}}{(\lambda^2+\mathbf{k}^2)^{\alpha/2}}\\&=\frac{1}{2^{(N+\alpha-2)}/2\pi^{N/2}\lambda^{\alpha-N}\Gamma(\alpha/2)}\\&\quad\times(\lambda\|\mathbf{r}-\mathbf{r}'\|)^{(\alpha-N)/2}K_{(N-\alpha)/2}(\lambda\|\mathbf{r}-\mathbf{r}'\|),\end{aligned} \tag{16}$$

where Γ is the Gamma function and $K_{(N-\alpha)/2}$ denotes the modified Bessel function of the third kind of order $(N-\alpha)/2$.

The RK $\Lambda_\alpha(\mathbf{r},\mathbf{r}')$ is an important kernel function which was first investigated in potential theory where it is termed the Bessel potential due to $K_{(N-\alpha)/2}$ [31]. The Appendix lists some of its basic properties relevant to this paper. In potential theory, the order parameter α in the kernel function $\Lambda_\alpha(\mathbf{r},\mathbf{r}')$ can be any positive real number. However, the Hilbert space associated with bound-state problems consists of the set of L^2 square-integrable functions and, accordingly, the corresponding RK also must be L^2 square integrable. Equations (A1) and (A4) show that the condition $\alpha>N$ must be fulfilled for the kernel function $\Lambda_\alpha(\mathbf{r},\mathbf{r}')$ to be bounded and L^2 square integrable. The positive definiteness of the symmetric kernel $\Lambda_\alpha(\mathbf{r},\mathbf{r}')$ is self-evident in the sense of Moore [26] [also see Eq. (19)]. It is important to point out that the value of the RK $\Lambda_\alpha(\mathbf{r},\mathbf{r}')$ depends only on the relative distance of two distinct points $\mathbf{r}$ and $\mathbf{r}'$, i.e., it is a radial basis function (RBF) and thus is rotationally invariant. Hereafter we adopt the form $\Lambda_\alpha(\|\mathbf{r}-\mathbf{r}'\|)$, under the name Sobolev RK of order α due to its relation to the operator $\hat{Q}_\alpha(\mathbf{r})$ [27], to indicate this radial property. The completion of the RKHS associated with $\Lambda_\alpha(\|\mathbf{r}-\mathbf{r}'\|)$ can be achieved with the same argument given for the 1D case [see the discussion below Eq. (10)]. Moreover, an important feature of the Sobo-

lev RK $\Lambda_\alpha(\|\mathbf{r}-\mathbf{r}'\|)$ is its high-order differentiability resulting from an appropriate choice of the order parameter $\alpha > N$. Finally, it is easy to see that the previous 1D example is a special case of the new generalized version with $\alpha=4$ and $N=1$.

B. Function approximation by radial basis functions

In what follows we will show an optimal feature of interpolation and function approximation in terms of the RBF $\Lambda_\alpha(\|\mathbf{r}-\mathbf{r}'\|)$ and its corresponding RKHS $\mathbf{H}_\alpha$. Consider an arbitrary set of M distinct scattered points $X=\{\mathbf{r}_1, \mathbf{r}_2, \ldots, \mathbf{r}_M\}$ in $\mathbb{R}^N$ and the corresponding scattered data $F=\{f(\mathbf{r}_1), f(\mathbf{r}_2), \ldots, f(\mathbf{r}_M)\}$ for a function $f\in\mathbf{H}_\alpha$. Since the Sobolev RK $\Lambda_\alpha(\|\mathbf{r}-\mathbf{r}'\|)$ for any fixed $\mathbf{r}'$ (or $\mathbf{r}$) belongs to $\mathbf{H}_\alpha$, its translates $\{\Lambda_\alpha(\|\mathbf{r}-\mathbf{r}_i\|)\}_{i=1}^M$, over the data set X, span a data-dependent subspace of $\mathbf{H}_\alpha$. The interpolant S_f to f can then be constructed via the representation

$$S_f(\mathbf{r})=\sum_{i=1}^M c_i\Lambda_\alpha(\|\mathbf{r}-\mathbf{r}_i\|), \tag{17}$$

where the real coefficients $c_1, c_2, \ldots, c_M$ solve the linear system

$$f(\mathbf{r}_j)=\sum_{i=1}^M c_i\Lambda_\alpha(\|\mathbf{r}_j-\mathbf{r}_i\|), \quad j=1,2,\ldots,M, \tag{18}$$

provided that the symmetric interpolation matrix $\{\Lambda_\alpha(\|\mathbf{r}_j-\mathbf{r}_i\|)\}$ is nonsingular. It has been shown that as long as the RBF $\Lambda_\alpha(\|\mathbf{r}-\mathbf{r}'\|)$ is positive-definite in the sense of Moore, i.e., for any set of M complex numbers $\{a_i\}_{i=1}^M$,

$$\begin{aligned}\sum_{i,j=1}^M a_j^*\Lambda_\alpha(\|\mathbf{r}_j-\mathbf{r}_i\|)a_i &= \sum_{i,j=1}^M a_j^* a_i\langle\Lambda_\alpha(\|\mathbf{r}-\mathbf{r}_j\|), \\ &\quad \times\Lambda_\alpha(\|\mathbf{r}-\mathbf{r}_i\|)\rangle_{\mathbf{r}} \\ &= \left\langle \sum_{i=1}^M a_i\Lambda_\alpha(\|\mathbf{r}-\mathbf{r}_i\|), \sum_{i=1}^M a_i\Lambda_\alpha \right. \\ &\quad \left. \times(\|\mathbf{r}-\mathbf{r}_i\|)\right\rangle_{\mathbf{r}} \geqslant 0, \end{aligned} \tag{19}$$

where the reproducing property

$$\langle\Lambda_\alpha(\|\mathbf{r}-\mathbf{r}_j\|), \Lambda_\alpha(\|\mathbf{r}-\mathbf{r}_i\|)\rangle_{\mathbf{r}}=\Lambda_\alpha(\|\mathbf{r}_j-\mathbf{r}_i\|) \tag{20}$$

has been used in the RKHS $\mathbf{H}_\alpha$, then the interpolation matrix is always nonsingular and thus Eq. (18) is solvable [27,28]. Moreover, for an arbitrary interpolant W_f to f of the form

$$W_f(\mathbf{r})=\sum_{i=1}^M f(\mathbf{r}_i)u_i(\mathbf{r}), \tag{21}$$

where the scattered data set F is the same as that used in Eq. (18) and $\{u_i(\mathbf{r})\}_{i=1}^M$ is an arbitrary set of linearly independent square integrable functions, Schaback [33] has shown that the error bound for this general interpolation can be given by

$$|f(\mathbf{r})-W_f(\mathbf{r})|\leqslant\|f\|_{\mathbf{H}_\alpha}\|\varepsilon(\mathbf{r},u,X)\|_{\mathbf{H}_\alpha}. \tag{22}$$

Here $\|\cdots\|_{\mathbf{H}_\alpha}$ indicates the norm in $\mathbf{H}_\alpha$ determined by the inner product (12), and $\varepsilon(\mathbf{r},u,X)$ represents the error functional whose norm can be explicitly written as

$$\begin{aligned}\|\varepsilon(\mathbf{r},u,X)\|_{\mathbf{H}_\alpha}^2 &= \Lambda_\alpha(0)-2\sum_{i=1}^M u_i(\mathbf{r})\Lambda_\alpha(\|\mathbf{r}-\mathbf{r}_i\|) \\ &\quad +\sum_{i,j=1}^M u_i(\mathbf{r})u_j(\mathbf{r})\Lambda_\alpha(\|\mathbf{r}_j-\mathbf{r}_i\|). \end{aligned} \tag{23}$$

This formula allows for comparisons among various interpolants. To this end we can ask for an optimal choice of the set $\{u_i(\mathbf{r})\}_{i=1}^M$ that minimizes Eq. (23). The optimal solution $u_i^s(\mathbf{r})$ can be obtained by taking the variation of Eq. (23), i.e., $\delta\|\varepsilon(\mathbf{r},u,X)\|_{\mathbf{H}_\alpha}^2=0$, and this results in the linear system for $u_i^s(\mathbf{r})$

$$\sum_{j=1}^M \Lambda_\alpha(\|\mathbf{r}_j-\mathbf{r}_i\|)u_i^s(\mathbf{r})=\Lambda_\alpha(\|\mathbf{r}-\mathbf{r}_j\|), \quad j=1,2,\ldots,M. \tag{24}$$

Since $\Lambda_\alpha(\|\mathbf{r}-\mathbf{r}'\|)$ is positive-definite, as described in Sec. II A, Eq. (24) is solvable and its solution is unique. As a result, the optimal solution is found to be

$$u_i^s(\mathbf{r})=\sum_{k=1}^M(\Lambda_\alpha^{-1})_{ik}\Lambda_\alpha(\|\mathbf{r}-\mathbf{r}_k\|), \quad i=1,2,\ldots,M, \tag{25}$$

where $(\Lambda_\alpha^{-1})_{ik}$'s are the elements of the inverse interpolation matrix $\{\Lambda_\alpha(\|\mathbf{r}_j-\mathbf{r}_i\|)\}$. It is clear that $u_i^s(\mathbf{r})$'s fall into the subspace spanned by the translates of $\{\Lambda_\alpha(\|\mathbf{r}-\mathbf{r}_i\|)\}_{i=1}^M$ and certainly satisfy the Lagrangian type interpolation conditions (i.e., cardinal condition)

$$u_i^s(\mathbf{r}_j)=\delta_{ij}, \quad i,j,=1,2,\ldots,M, \tag{26}$$

where δ_{ij} is the Kronecker delta. Substituting this optimal solution Eq. (25) back into Eq. (21), we find that the general interpolant $W_f(\mathbf{r})$ becomes equivalent to the interpolant $S_f(\mathbf{r})$ in Eq. (17), as can be seen from the following

$$\begin{aligned}W_f(\mathbf{r}) &= \sum_{i=1}^M f(\mathbf{r}_i)u_i^s(\mathbf{r})=\sum_{i=1}^M f(\mathbf{r}_i)\sum_{k=1}^M(\Lambda_\alpha^{-1})_{ik}\Lambda_\alpha(\|\mathbf{r}_k-\mathbf{r}\|) \\ &= \sum_{k=1}^M c_k\Lambda_\alpha(\|\mathbf{r}-\mathbf{r}_k\|)=S_f(\mathbf{r}), \end{aligned} \tag{27}$$

where $c_k=\Sigma_{i=1}^M f(\mathbf{r}_i)(\Lambda_\alpha^{-1})_{ik}$ is simply the unique solution of Eq. (18).

We come to the important conclusion that the interpolant $S_f(\mathbf{r})$ by the RBF $\Lambda_\alpha(\|\mathbf{r}-\mathbf{r}'\|)$ to scattered data is the unique minimizer of the error bound Eq. (22) among all general interpolants $W_f(\mathbf{r})$'s. Note that the error bound Eq. (22) is in reference to the RKHS $\mathbf{H}_\alpha$ which requires that $\hat{Q}_\alpha(\mathbf{r})f$ be square integrable (see Sec. II A).

III. NUMERICAL IMPLEMENTATION

This section describes the computational details for solving the bound-state Schrödinger equation by using the Sobolev RK $\Lambda_\alpha(\|\mathbf{r}-\mathbf{r}'\|)$. The underlying principle is to use the Sobolev RK $\Lambda_\alpha(\|\mathbf{r}-\mathbf{r}'\|)$ associated with the RKHS $\mathbf{H}_\alpha$ to approximate the wave function $\psi(\mathbf{r})$. There are two significant differences between the Sobolev RK $\Lambda_\alpha(\|\mathbf{r}-\mathbf{r}'\|)$ and the Gaussian function $\exp\{-\lambda(\mathbf{r}-\mathbf{r}')^2\}(\lambda>0)$ as interpolation bases. For fixed parameter $\alpha>N$, $\Lambda_\alpha(\|\mathbf{r}-\mathbf{r}'\|)$ is finitely continuously differentiable while $\exp\{-\lambda(\mathbf{r}-\mathbf{r}')^2\}(\lambda>0)$ is infinitely continuously differentiable. Numerical experiments have shown [27] that the condition number, defined as the ratio of largest and smallest eigenvalues of the interpolation matrix in Eq. (18), is generally large for infinitely differentiable (smooth) radial basis functions such as the Gaussian, when compared to finitely differentiable (smooth) ones such as the Sobolev RK. The larger the condition number is, the worse the approximation becomes. Moreover, for general bound-state problems with the potential having the property $V(\mathbf{r})\to 0$ at $\|\mathbf{r}\|\to\infty$, the correct asymptotic behavior of solutions of the Schrödinger equation has been explicitly built into the Sobolev RK, and the parameter λ appearing in $\Lambda_\alpha(\|\mathbf{r}-\mathbf{r}'\|)$ is related to the energy cutoff because the operator $\hat{M}_\alpha(\mathbf{r})=-\nabla_\mathbf{r}^2+\lambda^2$ [see Eq. (2)] is the asymptotic form of the Hamiltonian at large distances. However, the Gaussian function does not possess this property.

In general, the exact values of wave function $\psi(\mathbf{r})$ to be sought are not known on the grid points, nevertheless, the interpolant $S_f(\mathbf{r})$ as an expansion of data dependent (i.e., distributed) Sobolev RK $\Lambda_\alpha(\|\mathbf{r}-\mathbf{r}_i\|)$, $i=1,2,\ldots,M$, can be considered as an ansatz for the wave function $\psi(\mathbf{r})$. To determine the expansion coefficients $\{c_i\}$ of $\psi(\mathbf{r})$, instead of using the linear system Eq. (18), we can invoke the conventional Rayleigh-Ritz variational principle and solve the following linear system:

$$\sum_{j=1}^{M}(H_{ij}-ES_{ij})c_j=0,\quad i=1,2,\ldots,M, \tag{28}$$

where $H_{ij}=T_{ij}+V_{ij}$ and S_{ij} are the Hamiltonian and overlap matrix elements, respectively. The solution of the generalized linear eigenvalue problem in Eq. (28) will give the expansion coefficients and corresponding energy eigenvalues. As with other grid methods, the number of energy levels of Eq. (28) can be determined by properly setting an energy cutoff. The overlap matrix element S_{ij} and the kinetic matrix element T_{ij} can be easily worked out through the Fourier transform of the Sobolev RK. In terms of the definitions of S_{ij} and T_{ij}, we obtain their closed forms

$$\begin{aligned}S_{ij}&=C_\mu\int_{\mathbb{R}^N}d\mathbf{r}\Lambda_\alpha(\|\mathbf{r}-\mathbf{r}_i\|)*\Lambda_\alpha(\|\mathbf{r}-\mathbf{r}_j\|)\\&=\frac{C_\mu}{(2\pi)^N}\int_{\mathbb{R}^N}d\mathbf{k}\frac{e^{i\mathbf{k}\cdot(\mathbf{r}_i-\mathbf{r}_j)}}{(\lambda^2+\mathbf{k}^2)^\alpha}=C_\mu\Lambda_{2\alpha}(\|\mathbf{r}_i-\mathbf{r}_j\|)\end{aligned} \tag{29}$$

and

$$\begin{aligned}T_{ij}&=-\frac{C_\mu}{2}\int_{\mathbb{R}^N}d\mathbf{r}\Lambda_\alpha(\|\mathbf{r}-\mathbf{r}_i\|)*\nabla_\mathbf{r}^2\Lambda_\alpha(\|\mathbf{r}-\mathbf{r}_j\|)\\&=\frac{1}{2}\frac{C_\mu}{(2\pi)^N}\int_{\mathbb{R}^N}d\mathbf{k}\frac{\mathbf{k}^2e^{i\mathbf{k}\cdot(\mathbf{r}_i-\mathbf{r}_j)}}{(\lambda^2+\mathbf{k}^2)^\alpha}=\frac{C_\mu}{2}[\Lambda_{2\alpha-2}(\|\mathbf{r}_i-\mathbf{r}_j\|)\\&\quad-\lambda^2\Lambda_{2\alpha}(\|\mathbf{r}_i-\mathbf{r}_j\|)],\end{aligned} \tag{30}$$

where $C_\mu=(\Pi_{i=1}^N\sqrt{\mu_i})^{-1}$.

The remaining part of the present method involves the evaluation of the potential matrix elements V_{ij}, which is generally more cumbersome when compared to the DVR and other pseudospectral methods, or even the DGB. However, in terms of an intergral representation

$$\begin{aligned}\Lambda_\alpha(\|\mathbf{r}-\mathbf{r}'\|)&=\frac{1}{2^N\pi^{N/2}\lambda^{\alpha-N}\Gamma(\alpha/2)}\int_0^\infty dw w^{(\alpha-N)/2-1}\\&\quad\times\exp\left(-w-\frac{\lambda^2(\mathbf{r}-\mathbf{r}')^2}{4w}\right)\end{aligned} \tag{31}$$

for the Sobolev RK, these matrix elements can be conveniently expressed as the following integral:

$$\begin{aligned}V_{ij}&=C_\mu\int_{\mathbb{R}^N}d\mathbf{r}V(\mathbf{r})\Lambda_\alpha(\|\mathbf{r}-\mathbf{r}_i\|)*\Lambda_\alpha(\|\mathbf{r}-\mathbf{r}_j\|)\\&=B\int_0^{\pi/2}d\varphi\sin^{\alpha-1}(2\varphi)\int_0^\infty dw w^{(2\alpha-N)/2-1}\\&\quad\times\exp\left(-w-\frac{\lambda^2(\mathbf{r}_i-\mathbf{r}_j)^2}{4w}\right)\\&\quad\times\int_{\mathbb{R}^N}d\mathbf{r}e^{-\lambda^2\mathbf{r}^2}V[\mathbf{r}\sqrt{w}\sin(2\varphi)+\mathbf{r}_i\sin^2(\varphi)\\&\quad+\mathbf{r}_j\cos^2(\varphi)],\end{aligned} \tag{32}$$

where $B=C_\mu/[2^{N+\alpha-2}\pi^N\lambda^{2\alpha-2N}\Gamma(\alpha/2)^2]$, which can be analytically integrated for any polynomial potential. Explicitly, V_{ij} will be a combination of the Sobolev RK's of different orders [see, e.g., Eq. (38)].

In general, the evaluation of non-polynomial potential matrix elements requires numerical integration. However, unlike most existing grid methods, e.g., DVR and other pseudospectral methods, which assume fixed quadrature point distributions, the RBF based methods have no restriction on the grid point distributions as long as the condition number of the associated interpolation matrix $\{\Lambda_\alpha(\|\mathbf{r}_i-\mathbf{r}_j\|)\}$ is numerically acceptable. Consequently, we can judiciously arrange the grid points to match the symmetry of the potential and to have the significant regions covered by denser points. This added freedom of distributing grid points can lead to a substantial reduction of the total number of grid points used in the calculations, and thus reduce the computational cost, while still maintaining the desired numerical accuracy, as demonstrated in the following 1D and 2D examples.

Finally, we remark that the accuracy and efficiency of the present method depends on three factors: (1) the order parameter α which determines the size of the RKHS $\mathbf{H}_\alpha$ to be used in the formulation of a bound-state problem and the

exponential parameter λ of the RK $\Lambda_\alpha(\|\mathbf{r}-\mathbf{r}'\|)$ which is connected with the energy cutoff, (2) the number of the grid points which defines the size of a subspace of $\mathbf{H}_\alpha$ constructed from placing the Sobolev RK's on grids, (3) the distribution of grid points. All three factors are implicit in the interpolation condition Eq. (18), and hence the condition number of the interpolation matrix becomes a key measure for numerical accuracy and stability.

A. The 1D Morse potential

The numerical implementation in this first test is performed for the 1D Morse potential $V(x)=D(e^{-\beta x}-1)^2$ whose parameters are taken to be $D=0.1744$ a.u., $\beta=1.02764$ a.u., and $\mu=918.491$ a.u. to support 17 bound-state energy levels. Although the Morse potential is nonpolynomial, a proper choice of the order parameter α in the Sobolev RK $\Lambda_\alpha(\sqrt{\mu}|x-x'|)$ can allow for the potential matrix elements to be evaluated analytically. It is known [32] that the modified Bessel function of the third kind involved in the Sobolev RK will become a polynomial of $(\sqrt{\mu}|x-x'|)^{-1}$ times an exponential decaying factor of $\sqrt{\mu}|x-x'|$ if its index takes on half integers. Taking advantage of this observation and letting $(\alpha-1)/2=m+1/2$, $m=0,1,2,\ldots$, which clearly satisfies the condition $\alpha>1$, the Sobolev RK becomes

$$\Lambda_{2m+2}(\sqrt{\mu}|x-x'|) = \frac{\exp(-\lambda\sqrt{\mu}|x-x'|)}{2^{m+1}m!\lambda^{2m+1}}\sum_{k=0}^{m}\frac{(m+k)!}{k!(m-k)!2^k} \times(\lambda\sqrt{\mu}|x-x'|)^{m-k}, \tag{33}$$

and the potential matrix elements V_{ij} will then involve the integrals

$$\int_{-\infty}^{\infty}dx V(x)|x-x_i|^{m-k}|x-x_j|^{m-k'} \times\exp\{-\lambda\sqrt{\mu}(|x-x_i|+|x-x_j|)\}, \tag{34}$$

which can be integrated analytically to give a closed form. Note that, to obtain convergent integrals Eq. (34) for the Morse potential, the parameter λ in the Sobolev RK must be chosen such that $\lambda\sqrt{\mu}>\beta$.

Due to the asymmetrical nature of the Morse potential about its minimum $(z=0)$, the following simple formula:

$$x_i=-d_1\left(\frac{M_1-i}{M_1-1}\right)^{b_1},\quad i=1,2,\ldots,M_1,\quad x\leq 0,$$
$$x_{i+M_1}=d_2\left(\frac{i}{M-M_1}\right)^{b_2},\quad i=1,2,\ldots,M_2,\quad x>0 \tag{35}$$

is employed to distribute the grid points for the eigenvalue calculations instead of the semiclassically distributed grid points adopted by the DGB method [13]. Here $M=M_1+M_2$ is the total number of grid points used. M_2 and M_1 (including the potential minimum point) are the numbers of grid points allotted to the right- and the left-hand sides of the potential minimum (i.e., $x=0$), respectively. The truncated interval $[-d_1,d_2]$ in the calculations is defined in terms of the distances d_1 and d_2 from the potential minimum to the left and right endpoints of the interval, respectively. These distances are determined by the energy cutoff $E_{\rm cut}$ via the relations

$$d_1=\frac{1.8}{\beta}\ln\left(1+\sqrt{\frac{E_{\rm cut}}{D}}\right),$$
$$d_2=-\frac{1}{\beta}\ln\left(1-\sqrt{\frac{E_{\rm cut}}{D}}\right). \tag{36}$$

To calculate all 17 energy levels, the energy cutoff $E_{\rm cut}$ can be chosen to approach the dissociation limit. To be precise, we require $0.9999D\leq E_{\rm cut}<D$ to assure that $E_{\rm cut}$ lies above the last energy level. The exponents b_1,b_2 in Eq. (35) are independent of $E_{\rm cut}$ and are allowed to change over extensive ranges depending on the condition number of the interpolation matrix. Moreover, their values determine different distributions for a given set of grid points and energy cutoff.

The variational characteristic of the method allows us to minimize each calculated eigenvalue by varying the aforementioned three factors. For comparison, similar calculations were also done for the Gaussian radial basis function for which the grid points are distributed according to Eq. (36) instead of semiclassically chosen points because for more than one-dimensional cases no means is available to determine semiclassical grid points. Table I shows the values of the corresponding parameters adopted in the calculations as well as the exact eigenvalues of the Morse potential. Table II presents the calculated eigenvalues of the 1D Morse potential based on the parameters listed in Table I for the Gaussian radial basis function and the Sobolev RK. It is evident that the order of the Sobolev RK $\Lambda_\alpha(\sqrt{\mu}|x-x'|)$, in the present case, $\alpha=2(m+1)$, and the number of grid points, have significant effects on the accuracy of the method. The rate of convergence of the present method is very fast with increasing order α of $\Lambda_\alpha(\sqrt{\mu}|x-x'|)$ and the number of grid points. However, we also observed that a numerical trade-off has to be made between the smoothness of a RBF and the number of grid points. These two factors have tremendous influence on the condition number of the interpolation matrix by RBF. As mentioned above, the condition number of a low-order differentiable RBF is usually smaller than a high-order one, but more grid points are needed to improve the relative accuracy. Nevertheless, with an increase in the number of grid points, the linear dependence among RBF's distributed on the grids will dominate and cause a large condition number of the interpolation matrix. The Sobolev RK has more flexibility to control the condition number than the Gaussian radial basis function through the adjustment of its differentiability determined by the parameter α. For this 1D Morse potential, the calculated eigenvalues will become worse for different distributions of grid points when $m>9$ or $\alpha>20$. In addition, we also found that the results based on the Gaussian radial basis function is very sensitive and unstable with respect to the change of its exponential parameter as indicated by Franke in his classic paper [36] regarding RBF interpolation, but the Sobolev RK allows for a wider

TABLE I. Parameters and exact eigenvalues used in the calculations for the 1D Morse potential.

	Present work[a]					DGB[a]		
	$M=51$	$M=61$		$M=71$		$M=51$	$M=61$	$M=71$
	$m=7$	$m=5$	$m=7$	$m=4$	$m=6$			
λ	0.351	0.419	0.296	0.260	0.353	0.650	0.750	1.000
b_1	1.00	1.10	1.10	1.05	1.15	1.10	1.10	1.10
b_2	1.65	1.53	1.62	1.64	1.60	1.40	1.40	1.35
E_{cut}/D	0.99995	0.99993	0.999989	0.999989	0.999996	0.99995	0.999988	0.999994

v	Eigenvalue (a.u.)	v	Eigenvalue (a.u.)
0	0.009869224104150	12	0.160498622410143
1	0.028745352510513	13	0.165577633985531
2	0.046471721180962	14	0.169506885825004
3	0.063048330115496	15	0.172286377928562
4	0.078475179314116	16	0.173916110296205

[a] M_1 is fixed to be 11.

variation of its exponential parameter while maintaining the same numreical accuracy. Table II shows that the Sobolev RK can consistently yield better results than the Gaussian basis.

B. The 2D Henon-Heiles potential

The commonly used form of the 2D Henon-Heiles potential in atomic units is

$$V_{\text{HH}}(x,y)=\frac{1}{2}(x^2+y^2)+\gamma\left(x^2-\frac{1}{3}y^2\right)y \tag{37}$$

which implies that the mass $\mu=1$ and the fundamental frequency $\omega=1$ have been taken in the Hamiltonian of the system. Its ''dissociation energy'' is given by $E_d=(6\gamma^2)^{-1}$. In the following calculations the parameter $\gamma=\sqrt{0.0125}$ is adopted and accordingly, $E_d=40/3=13\frac{1}{3}$.

As discussed above, the present method places no stringent restriction on grid point distributions so that any appropriate 2D grid point sets can be used for solving the bound-state problem of the Henon-Heiles potential as long as the condition number of the interpolation matrix in Eq. (18) is numerically acceptable. Moreover, the inclusion of the potential symmetry in both the grid distribution and the interpolant $S_f(\mathbf{r})$ in Eq. (17) can greatly improve the numerical efficiency and accuracy, particularly for the treatment of degenerate energy levels. In view of the C_{3v} symmetry of the 2D Henon-Heiles potential, three types of the grid point distributions were used in a previous paper [35] for solving the bound-state Schrödinger equation by the collocation method in conjunction with the use of inverse multiquadrics as radial basis functions. However, only the equilateral triangular distribution, as schematically shown in Fig. 1, is considered in the present calculations.

In terms of Eq. (32) the matrix elements for the Henon-Heiles potential can be evaluated to give the following

TABLE II. Comparsion of the eigenvalues (a.u.) calculated by the present method with the DGB method and the exact ones for the Morse potential.

v	$E_v^{\text{exact}}-E_v^{\text{cal}}$							
	DGB[a]			Present work[a]				
	$M=51$	$M=61$	$M=71$	$M=51$	$M=61$		$M=71$	
				$m=7$	$m=5$	$m=7$	$m=4$	$m=6$
0	$-2.1[-13]$	$-1.1[-15]$	$-1.6[-14]$	$-4.4[-14]$	$-7.8[-14]$	$-0.0[-16]$	$-2.8[-15]$	$-1.1[-16]$
1	$-6.9[-13]$	$-0.15[-12]$	$-0.20[-12]$	$-1.1[-12]$	$-9.0[-13]$	$-1.9[-15]$	$-3.7[-14]$	$-8.0[-16]$
2	$-1.1[-11]$	$-4.9[-12]$	$-9.5[-13]$	$-1.2[-11]$	$-5.3[-12]$	$-2.2[-14]$	$-2.7[-13]$	$-2.0[-14]$
3	$-2.7[-10]$	$-4.8[-11]$	$-1.4[-12]$	$-7.3[-11]$	$-2.1[-11]$	$-1.4[-13]$	$-1.3[-12]$	$-2.2[-13]$
4	$-2.2[-09]$	$-2.3[-10]$	$-3.4[-13]$	$-3.3[-10]$	$-6.1[-11]$	$-8.4[-13]$	$-4.9[-12]$	$-4.8[-13]$
12	$-1.7[-07]$	$-4.1[-08]$	$-8.7[-09]$	$-2.3[-08]$	$-4.2[-09]$	$-3.5[-09]$	$-3.0[-09]$	$-2.8[-10]$
13	$-2.6[-07]$	$-5.8[-08]$	$-7.7[-09]$	$-5.9[-09]$	$-5.3[-09]$	$-4.9[-09]$	$-3.9[-09]$	$-4.1[-10]$
14	$-3.5[-07]$	$-6.5[-08]$	$-6.0[-09]$	$-2.0[-08]$	$-5.8[-09]$	$-5.4[-09]$	$-4.3[-09]$	$-5.0[-10]$
15	$-3.7[-07]$	$-5.6[-08]$	$-4.2[-09]$	$-3.2[-08]$	$-5.1[-09]$	$-4.3[-09]$	$-3.8[-09]$	$-4.8[-10]$
16	$-3.5[-07]$	$-4.5[-08]$	$-7.4[-09]$	$-7.0[-08]$	$-6.4[-08]$	$-4.9[-09]$	$-4.2[-09]$	$-5.8[-10]$

[a] $[-R]$ means 10^{-R}.

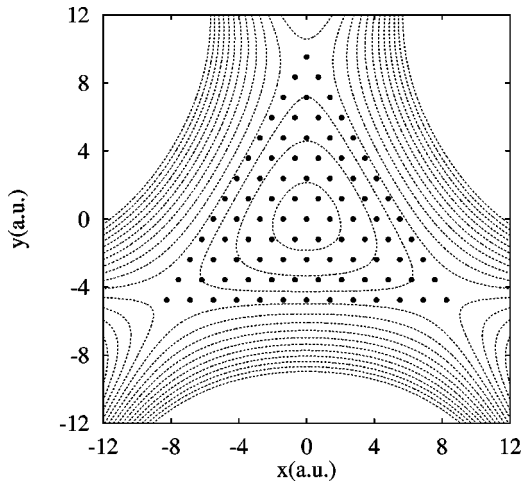

FIG. 1. Equilateral triangular domain with 91 uniformly distributed grid points. The dotted lines are the contours of the Henon-Heiles potential.

closed form:

$$(V_{\mathrm{HH}})_{ij}=\frac{C_\mu}{\alpha+1}\left\{\frac{\alpha^2}{2}\Lambda_{2\alpha+2}(\|\mathbf{r}_i-\mathbf{r}_j\|)+\Lambda_{2\alpha}(\|\mathbf{r}_i-\mathbf{r}_j\|)\right.$$
$$\times\left[2(V_{\mathrm{HH}}(x_i,y_i)+V_{\mathrm{HH}}(x_j,y_j))+\frac{\alpha}{2}\left(\frac{1}{2}(x_i+x_j)^2\right.\right.$$
$$\left.\left.\left.+(y_i+y_j)^2+V_{\mathrm{HH}}(x_i+x_j,y_i+y_j)\right)\right]\right\}. \qquad (38)$$

From Eqs. (29), (30), and (38), we immediately find that, by taking $\alpha-2=n+1/2$ with n a positive integer, the Sobolev RK's $\Lambda_{2\alpha-2}(\|\mathbf{r}_i-\mathbf{r}_j\|)$, $\Lambda_{2\alpha}(\|\mathbf{r}_i-\mathbf{r}_j\|)$, and $\Lambda_{2\alpha+2}(\|\mathbf{r}_i-\mathbf{r}_j\|)$ will become nth, $(n+1)$th, and $(n+2)$th order polynomials, of argument $\|\mathbf{r}_i-\mathbf{r}_j\|$, times a common exponential factor $e^{-\lambda\|\mathbf{r}_i-\mathbf{r}_j\|}$. This simple functional form allows us to freely choose the integer n to simplify the calculations, as seen in the 1D Morse potential case. In addition, a recursion relation can be established among $\Lambda_{2\alpha-2}(\|\mathbf{r}_i-\mathbf{r}_j\|)$, $\Lambda_{2\alpha}(\|\mathbf{r}_i-\mathbf{r}_j\|)$, and $\Lambda_{2\alpha+2}(\|\mathbf{r}_i-\mathbf{r}_j\|)$ in terms of the modified Bessel function of the third kind. This will result in a further reduction of computational work.

The numerical details with regard to the Henon-Heiles potential proceed as follows. (1) to cover all the bound-state energy levels, the energy cutoff for the calculations is taken to be $E_{\mathrm{cut}}=13.838642$ which is slightly larger than the ''dissociation energy'' $E_d=40/3=13\frac{1}{3}$ of the system. (2) The equilateral triangular grid domain is determined by this energy cutoff and grid points are distributed symmetrically and uniformly. (3) For the fixed order $\alpha-2=n+1/2$, the parameter λ in $\Lambda_\alpha(\|\mathbf{r}-\mathbf{r}'\|)$ is determined such that all the resulting energy levels are on average the lowest among all the calculations. In general, we have found that the calculated energy levels are not very sensitive to the change of λ over certain ranges. Table III lists the values of parameter λ used in the calculations and the corresponding range within which the calculated energy levels differ at most in their fifth decimal places. To investigate the convergence with respect to the order parameter $\alpha-2=n+1/2$ and the number of grid points M, we have carried out a series of calculations with $n=11-20$ and sets of 496, 595, and 703 grid points. Only the results corresponding to $n=17,20$ and the set of 595 grid points are shown in Table III. As a reference, we also calculated the case of $n=22$ with a set of 1081 grid points for convergence checks.

For comparison, also listed in Table III are the DAF's results [18] which use 2500 evenly spaced grid points and the DGB's results [13] based on the symmetry adapted linear combination of Gaussian radial basis functions located at 462 C_{3v} symmetrically distributed grid points. It is seen that the present results are in excellent agreement with the previous ones despite the interpolant $S_f(\mathbf{r})$ used in the calculation not being symmetrized according to the structure of the Henon-Heiles potential. In particular, we note that the absolute differences between the calculated double degenerate energies of the last energy level still stays as small as 10^{-10} in the case of $n=17$ and 595 grid points. The differences for lower degenerate energy levels are basically the same as the machine precision. Moreover, at a fixed n, the convergence of the calculated energy levels is very rapid with respect to the number of grid points, as demonstrated by the last five energy levels for $n=20$ and 496 grid points which are in agreement with the corresponding ones for $n=20$ and 595 grid points. In general, we found that the calculation is basically converged once the order $n=\alpha-5/2$ of the Sobolev RK $\Lambda_\alpha(\|\mathbf{r}-\mathbf{r}'\|)$ is beyond 17, but not more than 25. Overall results for the different choices are closer to that of DAF [18] than DGB [13].

Finally, unlike the DVR or its variants, the present method does not suffer from the occurrence of so-called ghost energy levels [37]. For example, we have also made a series of calculations using the Colbert-Miller DVR scheme [5], and the results are generally worse than ours and HL's presented in Table III. Specifically, the following is found. (1) A large number of grid points (at least 2000 points depending on different energy cutoffs) is always needed to cover the entire energy spectra below the ''dissociation limit.'' (2) The ghost energy levels frequently occur in the range of middle to high energy levels. It is difficult to recognize and discard them if there is no *a priori* knowledge about the correct energy spectra of the system under study. (3) The numerical resolution for degenerate energy levels are at least four orders of magnitude lower than in the present calculations.

IV. CONCLUSION

There are four remarkable features over the other existing methods in using the Sobolev RK to numerically solve bound-state problems. First, a function can be optimally recovered from scattered data by Sobolev RK interpolation. This feature assures the robustness of the method. Second, the Sobolev RK has more flexibility to control the condition number of the interpolation matrix through the adjustment of its differentiability determined by its order parameter α. This feature asssures the stability and accuracy of the method. Third, no special distribution for grid points and no tensor product ansatz for multidimensions are required, thus, allowing for a judicious choice of grid points according to the physical properties of the wave functions and potential under study as long as the condition number of the resulting inter-

TABLE III. Comparisons of the calculated eigenvalues for the Henon-Heiles potential.

State	HL [13]	DAF [18]	Present work[a]		
			$n=17$	$n=20$	$n=22$
			$M=595$	$M=595$	$M=1081$
			$\lambda=5.00\sim5.50$	$\lambda=5.40\sim7.80$	$\lambda=6.00\sim8.50$
$3A_1$	3.982417	3.982417	3.982417	3.982417	3.982417
$1A_2$	3.985761	3.985761	3.985761	3.985761	3.985761
$5A_1$	5.867015	5.867015	5.867015	5.867015	5.867015
$2A_2$	5.881447	5.881446	5.881446	5.881446	5.881446
$3A_2$	6.998932	6.998932	6.998932	6.998932	6.998932
$7A_1$	6.999387	6.999387	6.999387	6.999387	6.999387
$8A_1$	7.697722	7.697721	7.697721	7.697721	7.697721
$4A_2$	7.736884	7.736885	7.736885	7.736885	7.736885
$5A_2$	8.811326	8.811327	8.811327	8.811327	8.811327
$10A_1$	8.815189	8.815188	8.815188	8.815188	8.815188
$11A_1$	9.466775	9.466773	9.466773	9.466773	9.466773
$6A_2$	9.552382	9.552382	9.552382	9.552382	9.552382
$12A_1$	10.035414	10.035413	10.035413	10.035413	10.035413
$7A_2$	10.035594	10.035592	10.035592	10.035592	10.035592
$8A_2$	10.572478	10.572480	10.572480	10.572480	10.572480
$14A_1$	10.590478	10.590470	10.590470	10.590470	10.590470
$15A_1$	11.160260	11.160259	11.160259	11.160258	11.160258
$9A_2$	11.325231	11.325231	11.325232	11.325232	11.325231
$16A_1$	11.749558	11.749518	11.749519	11.749518	11.749518
$10A_2$	11.752298	11.752297	11.752297	11.752297	11.752297
$11A_2$	12.277191	12.277192	12.277193	12.277192	12.277192
$18A_1$	12.333799	12.333785	12.333781	12.333780	12.333778
$19A_1$	12.748313	12.748423	12.748197	12.748195	12.748190
$12A_2$	13.032057	13.032062	13.032064	13.032062	13.032061
$32E$	13.081194	13.081196	13.081196	13.081194	13.081192
$13A_2$	13.086874	13.086873	13.086874	13.086873	13.086873
$33E$	13.233287		13.233250	13.233249	13.233249

polation matrix is numerically acceptable. This feature assures the efficiency of the method. Finally, for general bound-state problems with a potential satisfying $V(\mathbf{r})\to 0$ at $\|\mathbf{r}\|\to\infty$, the correct asymptotic behavior of solutions to the Schrödinger equation has been explicitly built into the Sobolev RK. In addition, the variational characteristic of the method avoids the occurrence of so-called ghost energy levels which exist in the nonvariational methods such as DVR, etc. The results of the above two examples showed that the order α of the Sobolev RK $\Lambda_\alpha(\|\mathbf{r}-\mathbf{r}'\|)$ can approximately be set equal to 16 such that $(-\nabla^2+\lambda^2)^{\alpha/4}\psi(\mathbf{r})$ is square integrable, i.e., the corresponding RKHS's are composed of at least 8 times continuously differentiable square-integrable functions. Despite the Hamiltonian matrix not being sparse, its diagonalization is efficient due to its low dimension. The evaluation of the potential matrix elements V_{ij} in the present method remains a numerical challenge when dealing with general nonpolynomial potentials. For molecular bound-state problems studies are underway.

APPENDIX: MATHEMATICAL PROPERTIES OF $\Lambda_\alpha(\|\mathbf{r}-\mathbf{r}'\|)$

Most of the fundamental properties of the Sobolev RK (15) follow immediately from the corresponding properties of the modified Bessel function of the third kind $K_{(N-\alpha)/2}(\lambda\|\mathbf{r}-\mathbf{r}'\|)$ [32]. Here we only list a few relevant results.

The function $\Lambda_\alpha(\|\mathbf{r}-\mathbf{r}'\|)$ is analytic except at $\|\mathbf{r}-\mathbf{r}'\|=0$ and for $\|\mathbf{r}-\mathbf{r}'\|\neq 0$ it is an entire function of α. Its asymptotic properties as $\|\mathbf{r}-\mathbf{r}'\|\to 0$, are

$$\Lambda_\alpha(\|\mathbf{r}-\mathbf{r}'\|)\sim\begin{cases}\dfrac{\Gamma((\alpha-N)/2)}{2^N\pi^{N/2}\lambda^{\alpha-N}\Gamma(\alpha/2)} & \text{if } \alpha>N,\\ \dfrac{-\log(\lambda\|\mathbf{r}-\mathbf{r}'\|)}{2^{N-1}\pi^{N/2}\Gamma(N/2)} & \text{if } \alpha=N,\\ \dfrac{\Gamma((N-\alpha)/2)(\|\mathbf{r}-\mathbf{r}'\|)^{\alpha-N}}{2^\alpha\pi^{N/2}\Gamma(\alpha/2)} & \text{if } \alpha<N.\end{cases} \tag{A1}$$

Similarly for $\|\mathbf{r}-\mathbf{r}'\|\to\infty$,

$$\Lambda_\alpha(\|\mathbf{r}-\mathbf{r}'\|)\to\frac{(\lambda\|\mathbf{r}-\mathbf{r}'\|)^{(\alpha-N-1)/2}}{2^{(\alpha+N-1)/2}\pi^{(N-1)/2}\lambda^{\alpha-N}\Gamma(\alpha/2)}e^{-\lambda\|\mathbf{r}-\mathbf{r}'\|} \quad \text{for } \alpha>0. \tag{A2}$$

$\Lambda_\alpha(\|\mathbf{r}-\mathbf{r}'\|)$ is integrable for any $\alpha>0$ and any given $\mathbf{r}$ (or $\mathbf{r}'$), i.e.,

$$\int_{\mathbb{R}^N} d\mathbf{r}'\,\Lambda_\alpha(\|\mathbf{r}-\mathbf{r}'\|)=\int_{\mathbb{R}^N} d\mathbf{r}\Lambda_\alpha(\|\mathbf{r}-\mathbf{r}'\|)=\tilde{\Lambda}_\alpha(0)=\lambda^{-\alpha}. \tag{A3}$$

But it is not necessarily square integrable unless $\alpha>N/2$ for any given $\mathbf{r}$ (or $\mathbf{r}'$), i.e.,

$$\int_{\mathbb{R}^N} d\mathbf{r}'\,\Lambda_\alpha(\|\mathbf{r}-\mathbf{r}'\|)^*\Lambda_\alpha(\|\mathbf{r}-\mathbf{r}'\|)=\Lambda_{2\alpha}(0)$$

$$=\begin{cases} \dfrac{\Gamma(\alpha-N/2)}{2^N\pi^{N/2}\lambda^{2\alpha-N}\Gamma(\alpha)} & \text{if } \alpha>N/2, \\ \lim\limits_{\mathbf{r}\to 0}\dfrac{-\log(\lambda\|\mathbf{r}\|)}{2^{N-1}\pi^{N/2}\Gamma(N/2)} & \text{if } \alpha=N/2, \\ \lim\limits_{\mathbf{r}\to 0}\dfrac{\Gamma(N/2-\alpha)\|\mathbf{r}\|^{2\alpha-N}}{2^{2\alpha}\pi^{N/2}\Gamma(\alpha)} & \text{if } \alpha<N/2. \end{cases} \tag{A4}$$

It is apparent that the integrals diverge for $\alpha\leqslant N/2$.

For any given $\alpha,\alpha'>0$, the composition formula holds for the Sobolev RK, i.e.,

$$\Lambda_{\alpha+\alpha'}(\|\mathbf{r}\|)=\Lambda_\alpha^*\Lambda_{\alpha'}(\|\mathbf{r}\|)=\int_{\mathbb{R}^N} d\mathbf{r}'\,\Lambda_\alpha(\mathbf{r})\Lambda_{\alpha'}(\|\mathbf{r}-\mathbf{r}'\|). \tag{A5}$$

For fixed $\mathbf{r}'$ and $\mathbf{r}\neq\mathbf{r}'$, an important differential relationship between the Sobolev RK and the operator $\hat{M}(\mathbf{r})$ exists as follows:

$$\hat{M}(\mathbf{r})\Lambda_\alpha(\|\mathbf{r}-\mathbf{r}'\|)=(-\nabla_{\mathbf{r}}^2+\lambda^2)\Lambda_\alpha(\|\mathbf{r}-\mathbf{r}'\|)$$
$$=\Lambda_{\alpha-2}(\|\mathbf{r}-\mathbf{r}'\|). \tag{A6}$$

As a corollary one has for all positive integer $m<\alpha/2$

$$(-\nabla_{\mathbf{r}}^2+\lambda^2)^m\Lambda_\alpha(\|\mathbf{r}-\mathbf{r}'\|)=\Lambda_{\alpha-2m}(\|\mathbf{r}-\mathbf{r}'\|). \tag{A7}$$

It is obvious that the function $\Lambda_{2m}(\|\mathbf{r}-\mathbf{r}'\|)$ is a fundamental solution for the operator $(-\nabla^2+\lambda^2)^m$.

ACKNOWLEDGMENT

The authors acknowledge support from the Department of Energy.

[1] *Numerical Grid Methods and Their Applications to Schödinger Equation*, edited by C. Cerjan (Kluwer Academic, Dordrecht 1993).

[2] J. C. Light, I. P. Hamilton, and J. V. Lill, J. Chem. Phys. **82**, 1400 (1985).

[3] D. Baye and P. H. Heenen, J. Phys. A **19**, 2041 (1986).

[4] J. T. Muckerman, Chem. Phys. Lett. **173**, 200 (1990).

[5] D. T. Colbert and W. H. Miller, J. Chem. Phys. **96**, 1982 (1992).

[6] B. S. Shizgal and H. Chen, J. Chem. Phys. **104**, 4137 (1996).

[7] B. I. Schneider, Phys. Rev. A **55**, 3417 (1997).

[8] H. Karabulut and E. L. Silbert III, J. Phys. A **30**, L513 (1997).

[9] D. Gottlieb and S. A. Orszag, *Numerical Analysis of Spectral Methods: Theory and Applications*, 3rd. Printing (SIAM, Philadelphiia, 1983).

[10] R. Kosloff, in *Dynamics of Molecules and Chemical Reactions*, edited by R. E. Wyatt and J. Z. H. Zhang (Marcel Dekker, New York, 1996).

[11] B. W. Shore, J. Chem. Phys. **59**, 6450 (1973).

[12] M. J. Davis and E. J. Heller, J. Chem. Phys. **71**, 3383 (1979).

[13] I. P. Hamilton and J. C. Light, J. Chem. Phys. **84**, 306 (1986).

[14] W. Yang and A. C. Peet, Chem. Phys. Lett. **153**, 98 (1988).

[15] Z. Bačić and J. C. Light, Annu. Rev. Phys. Chem. **40**, 469 (1989).

[16] G. W. Wei, D. S. Zhang, D. J. Kouri, and D. K. Hoffman, Phys. Rev. Lett. **79**, 775 (1997).

[17] D. K. Hoffman, G. W. Wei, D. S. Zhang, and D. J. Kouri, Phys. Rev. E **57**, 6152 (1997), and references therein.

[18] D. S. Zhang, G. W. Wei, D. J. Kouri, and D. K. Hoffman, J. Chem. Phys. **106**, 5216 (1996).

[19] D. K. Hoffman, T. L. Marchioro II, M. Arnold, Y. Huang, W. Zhu, and D. J. Kouri, J. Math. Chem. **20**, 117 (1994).

[20] T.-S. Ho and H. Rabitz, J. Chem. Phys. **104**, 2584 (1995); **105**, 10 472 (1996).

[21] T. Hollebeek, T.-S. Ho, and H. Rabitz, J. Chem. Phys. **106**, 7223 (1997).

[22] G. C. Schatz, A. Papaionnou, L. A. Pederson, L. R. Harding, T. Ho Hebeek, T.-S. Ho, and H. Rabitz, J. Chem. Phys. **107**, 2340 (1997).

[23] H.-G. Hu, T.-S. Ho, and H. Rabitz, Chem. Phys. Lett. **288**, 719 (1998).

[24] C. de Boor and R. E. Lynch, J. Math. Mech. **15**, 953 (1966).

[25] G. Wahba, *Spline Models for Observational Data* (SIAM, Philadelphia, 1990).

[26] N. Aronszajn, Trans. Am. Math. Soc. **68**, 337 (1950).

[27] R. Schaback, in Vol. 1 of *Approximation and Interpolation, Approximation Theory VII*, edited by C. K. Chui and L. L. Schumaker (World Scientific, Singapore, 1995), p. 491.

[28] N. J. D. Powell, in *Advances in numerical Analysis II: Wavelets, Subdivision Algorithms, and Radial Basis Functions*, edited by W. A. Light (Oxford University Press, Oxford, 1992), p. 105.

[29] M. H. Kalos, Phys. Rev. **128**, 1791 (1962); S. Zhang and M. H. Kalos, Phys. Rev. Lett. **67**, 3074 (1991).

[30] D. R. Adams and L. I. Hedberg, *Function Spaces and Potential Theory* (Springer-Verlag, Berlin, 1996).

[31] A. Aronszajn and K. T. Smith, Ann. Inst. Fourier **11**, 385 (1961).

[32] I. S. Gradshteyn and I. M. Ryzhik, *Table of Integrals, Series, and Products* (Academic, New York, 1980).

[33] R. Schaback, Ann. Numer. Math. **4**, 537 (1997).
[34] R. Schaback, in *Multivariate Approximations: From CAGD to Wavelets*, edited by K. Jetter and F. Utreras (World Scientific, Singpore, 1993), p. 293.
[35] X.-G. Hu, T.-S. Ho, and H. Rabitz, Comput. Phys. Commun. **113**, 168 (1998).
[36] R. Franke, Math. Comput. **38**, 181 (1982).
[37] H. Wei, J. Chem. Phys. **106**, 6885 (1997).